

MEASUREMENTS OF BEAM HALO DIFFUSION AND POPULATION DENSITY IN THE TEVATRON AND IN THE LARGE HADRON COLLIDER*

G. Stancari[†], Fermilab, Batavia, IL 60510, USA

Abstract

Halo dynamics influences global accelerator performance: beam lifetimes, emittance growth, dynamic aperture, and collimation efficiency. Halo monitoring and control are also critical for the operation of high-power machines. For instance, in the high-luminosity upgrade of the LHC, the energy stored in the beam tails may reach several megajoules. Fast losses can result in superconducting magnet quenches, magnet damage, or even collimator deformation. The need arises to measure the beam halo and to remove it at controllable rates. In the Tevatron and in the LHC, halo population densities and diffusivities were measured with collimator scans by observing the time evolution of losses following small inward or outward collimator steps, under different experimental conditions: with single beams and in collision, and, in the case of the Tevatron, with a hollow electron lens acting on a subset of bunches. After the LHC resumes operations, it is planned to compare measured diffusivities with the known strength of transverse damper excitations. New proposals for nondestructive halo population density measurements are also briefly discussed.

INTRODUCTION

Understanding particle losses and beam quality degradation is one of the fundamental aspects in the design and operation of accelerators. From the point of view of machine protection, losses must be absorbed by the collimation system to avoid damaging components. Beam lifetimes and emittance growth determine the luminosity of colliders. Knowledge of the machine aperture (physical and dynamical) and of the mechanisms that drive particle loss is essential.

The LHC and its planned luminosity upgrades (HL-LHC) represent huge leaps in the stored beam energy of colliders. In 2011, the Tevatron stored a beam of 2 MJ at 0.98 TeV, whereas the LHC reached 140 MJ in 2012 at 4 TeV. The nominal LHC will operate at 362 MJ at 7 TeV in 2015, and the HL-LHC project foresees that around 2023 the machine will store proton beams of 692 MJ.

No scrapers exist in the LHC for full beam at top energy. Moreover, the minimum design HL-LHC lifetimes (about 0.2 h for slow losses during squeeze and adjust) are

close to the plastic deformation of primary and secondary collimators.

Halo populations in the LHC are not well known. Collimator scans [1, 2], van-der-Meer luminosity scans [3], and losses during the ramp [4] indicate that the tails above 4σ (where σ is the transverse rms beam size) represent between 0.1% and 2% of the total population, which translates to megajoules of beam at 7 TeV. Quench limits, magnet damage, or even collimator deformation will be reached with fast losses [5]. In HL-LHC, these fast losses include crab-cavity failures, which generate orbit drifts of about 2σ [6].

Hence, the need arises to measure and monitor the beam halo, and to remove it at controllable rates. For HL-LHC, beam halo monitoring and control are one of the major risk factors for operation with crab cavities. Hollow electron lenses were proposed as an established and flexible tool for controlling the halo of high-power beams [7].

The dynamics of particles in an accelerator can be quite complex. Deviation from linear dynamics can be large, especially in the beam halo. Lattice resonances and nonlinearities, coupling, intrabeam and beam-gas scattering, and the beam-beam force in colliders all contribute to the topology of the particles' phase space, which in general will include regular and chaotic regions, and resonant islands. In addition, various noise sources are present in a real machine, such as ground motion (resulting in orbit and tune jitter) and ripple in the radiofrequency and magnet power supplies. As a result, the macroscopic motion can acquire a stochastic character, which can be described in terms of particle diffusion [8–12].

Calculations of lifetimes, emittance growth rates, and dynamic aperture from various sources are routinely performed in the design stage of all major accelerators, providing the foundation for the choice of operational machine parameters. Experimentally, it was shown that beam halo diffusion can be measured by observing the time evolution of particle losses during a collimator scan [13]. These phenomena were used to estimate the diffusion rate in the beam halo in the SPS at CERN [14, 15], in HERA at DESY [13], and in RHIC at BNL [16]. An extensive experimental campaign was carried out at the Tevatron in 2011 [17–19] to characterize the beam dynamics of colliding beams and to study the effects of the novel hollow electron beam collimator concept [20]. Following the results of the Tevatron measurements, similar experiments were done in the LHC [2, 21].

In this paper, we review some of the present and future experimental methods to estimate beam halo populations, with a discussion of their systematic effects. We also survey the experimental data on the dynamics of the beam halo,

* Fermilab is operated by Fermi Research Alliance, LLC under Contract No. DE-AC02-07CH11359 with the United States Department of Energy. This work was partially supported by the US DOE LHC Accelerator Research Program (LARP) and by the European FP7 HiLumi LHC Design Study, Grant Agreement 284404. Report number: FERMILAB-CONF-14-450-AD-APC.

[†] Email: (stancari@fnal.gov).

with a discussion on the relationship between diffusivities and population densities.

HALO POPULATION DENSITY

Collimator scans

The dynamics of the beam halo was studied experimentally with collimator scans [13] at the Fermilab Tevatron proton-antiproton collider in 2011. The main motivation was to observe the effect on diffusion of beam-beam forces and of the novel hollow electron beam collimator [20]. The same data was used to estimate halo populations beyond about 7σ . Lower amplitudes could not be reached because of the minimum size of the collimator steps and of the safety thresholds of the beam loss monitors.

In the Tevatron, 36 proton bunches (identified as P1–P36) collided with 36 antiproton bunches (A1–A36) at the center-of-momentum energy of 1.96 TeV. There were 2 head-on interaction points (IPs), corresponding to the CDF and the DZero experiments. Each particle species was arranged in 3 trains of 12 bunches each, circulating at a revolution frequency of 47.7 kHz. The bunch spacing within a train was 396 ns, or 21 53-MHz rf buckets. The bunch trains were separated by 2.6- μ s abort gaps. The synchrotron frequency was 34 Hz, or 7×10^{-4} times the revolution frequency. The machine operated with betatron tunes near 20.58. Protons and antiprotons shared a common vacuum pipe. Outside of the interaction regions, their orbits wrapped around each other in a helical arrangement. Therefore, bunch centroids could be several millimeters away from the physical and magnetic axes of the machine. Beam intensities and bunch lengths were measured with a resistive wall monitor. Transverse beam sizes were inferred from the recorded synchrotron light images.

All collimators were retracted except one. The collimator of interest was moved in or out in small steps, and the corresponding local loss rates were recorded as a function of time. A detailed description of the Tevatron collimation system can be found in Ref. [22].

Collimator scans were also used to estimate halo populations in the LHC at 4 TeV. The experiments were described in Refs. [2, 21]. The goal of these experiments was to measure both halo populations and diffusivities under the same conditions. One nominal bunch (1.15×10^{11} protons) per beam was used. The study started with squeezed, separated beams. Orbit stabilization was turned off. The primary and secondary collimators in the IR7 region were retracted from their nominal settings of 4.3σ and 6.3σ respectively to a half gap of 7σ . The jaws of a vertical and a horizontal primary collimators were moved in small steps. The collimators were selected from different beams to be able to perform the scrapings in parallel without inducing cross-talk in the loss-monitor signals. The jaws were moved after waiting for the beam losses from the previous step to reach a steady-state (approximately every 10 to 40 seconds). The jaws were left for a few minutes in the beam after they had reached their final inward position, to allow the losses to

stabilize. Subsequently, the jaws were moved out in small steps, again after waiting for the transient to decay. The procedure of inward and outward steps was then repeated after bringing the beams into collision.

In the approximation of static beam distributions, the beam densities can be calculated from the measured intensity loss during a short interval (4 s in this case) centered around the collimator movement. The results are shown in Figure 1 (solid black lines). Similar results are obtained by integrating the calibrated losses over the same short interval (Figure 1, dashed black lines). For comparison, a Gaussian core with the measured beam emittance is also shown in Figure 1 (gray line). Tail populations beyond 4σ are reported in Table 1. It is interesting to note the depletion in the case of collisions compared with separated beams.

Scans with primary collimators in a dispersive region of the LHC were used to estimate the population of the off-momentum halo and of the abort gap [23]. Tails of about 0.5% were observed at a relative momentum deviation above 1×10^{-3} .

Other estimates

An estimate of the beam distribution can be obtained with van-der-Meer luminosity scans [3, 6]. The two colliding beams are displaced with respect to each other, and the luminosity is recorded as a function of separation. With this technique, it was observed that the luminosity curve is well described by a double Gaussian, and that the beam population above 4σ was of the order of 0.1%.

Losses during the LHC acceleration ramp, as the collimator settings are tightened, also give indications of the magnitude of beam tails [4]. On average, 1% of the beam was above 6σ and was lost during the ramp in 2012.

Nondestructive beam halo diagnostics

Halo monitoring is clearly a high priority for high-power machines. A true halo monitor should provide a real-time, 2-dimensional transverse beam distribution. This requires a response time of a few seconds, and a dynamic range of the order of 10^6 .

In the LHC, it is planned to use synchrotron radiation as diagnostic phenomenon [24]. Dynamic range can be achieved with the coronagraph technique [25] (perhaps replacing the stop with a neutral filter), or more simply with a set of state-of-the-art digital cameras.

A new kind of detector was recently developed for the RHIC electron lenses [26]. It was shown that the rate of electrons backscattered towards the gun by Coulomb collisions with the circulating ions is a sensitive probe of the overlap between the two beams. Although a 2-dimensional reconstruction would require some kind of scanning of the electron beam, the method is based on scintillator counters and has a wide dynamic range. It is a promising means to continuously monitor the halo, especially in conjunction with a hollow electron lens.

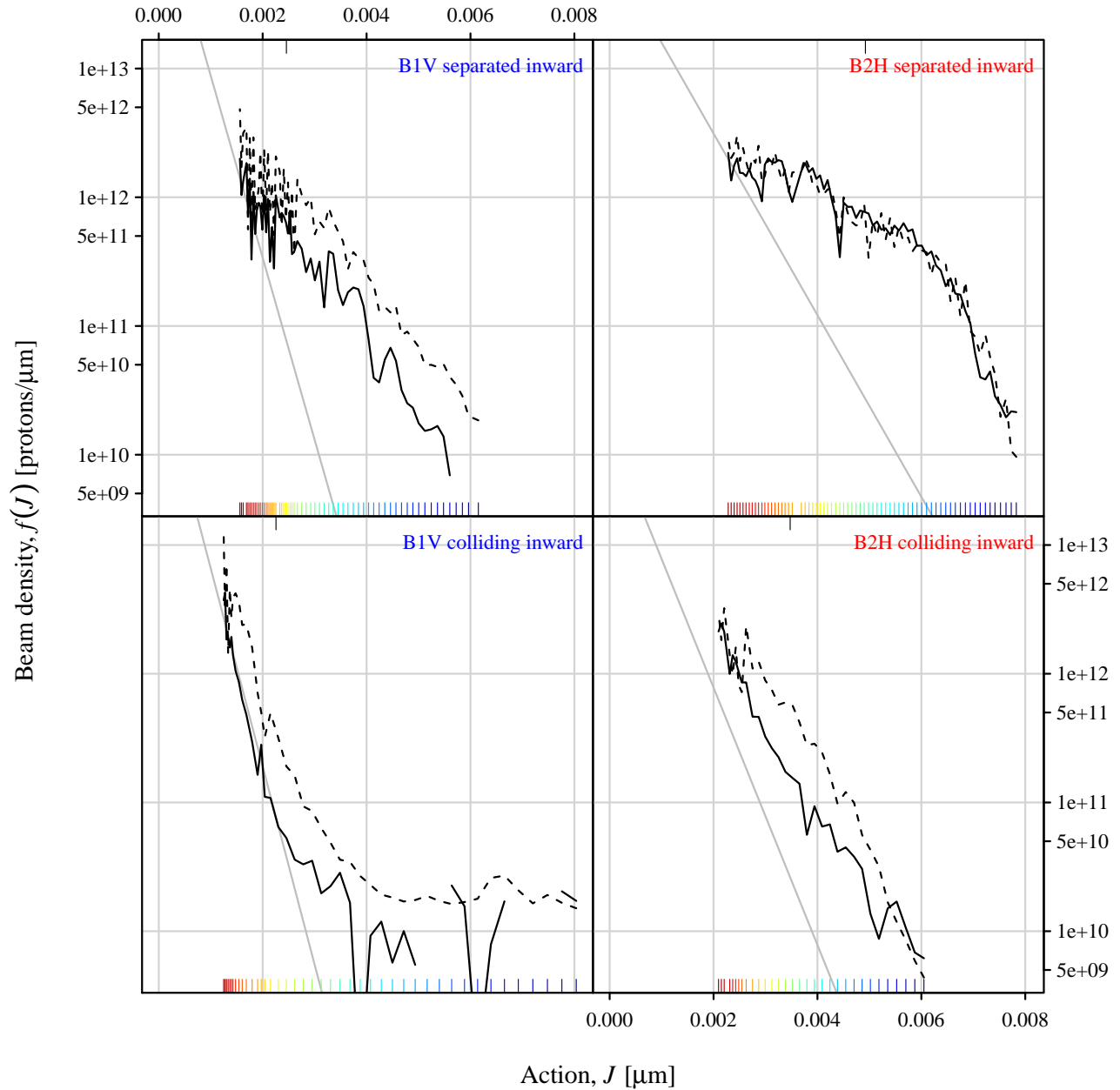


Figure 1: Measured beam halo distributions during the inward collimator scans in the LHC at 4 TeV, as a function of collimator position in units of action $J \equiv x_c^2 / (2\beta)$, where x_c is the half gap and β is the local amplitude lattice function: from total intensity loss (solid black); from integrated loss-monitor rates (dashed black). The gray line denotes a Gaussian core with the measured beam emittance. The colored vertical tick marks indicate the collimator positions. The 2 left plots refer to the vertical scraping of beam 1 with separated and colliding bunches; the 2 right plots are for beam 2 in the horizontal plane.

Table 1: Estimates of halo population in the LHC at 4 TeV with collimator scans.

Data set	Beam	Plane	Collisions?	Action J corresponding to 4σ [μm]	Tail population beyond 4σ [$10^8 p$]	[%]
1	B1	V	N	0.00246	8.2	0.58
2	B1	V	Y	0.00226	1.6	0.13
3	B2	H	N	0.00492	8.5	0.86
4	B2	H	Y	0.00347	2.4	0.35

HALO DIFFUSIVITY

Halo diffusivities can also be measured with collimator scans [13]. All collimators except one are retracted. As the collimator jaw of interest is moved in small steps (inward or outward), the local shower rates are recorded as a function of time. Collimator jaws define the machine aperture. If they are moved towards the beam center in small steps, typical spikes in the local shower rate are observed, which approach a new steady-state level with a characteristic relaxation time. When collimators are retracted, on the other hand, a dip in loss rates is observed, which also tends to a new equilibrium level.

We consider the evolution in time t of a beam of particles with density $f(J, t)$ described by the diffusion equation $\partial_t f = \partial_J (D \partial_J f)$, where J is the Hamiltonian action and D the diffusion coefficient in action space. The particle flux at a given location $J = \bar{J}$ is $\phi = -D \cdot [\partial_J f]_{J=\bar{J}}$. During a collimator step, the action $J_c = x_c^2 / (2\beta_c)$, corresponding to the collimator half gap x_c at a ring location where the amplitude function is β_c , changes from its initial value J_{ci} to its final value J_{cf} in a time Δt . In the Tevatron, typical steps in half gap were $50 \mu\text{m}$ in 40 ms; smaller steps ($10 \mu\text{m}$ in 5 ms, typically) were possible in the LHC. In both cases, the amplitude function was of the order of a hundred meters. It is assumed that the collimator steps are small enough so that the diffusion coefficient can be treated as a constant in that region. If D is constant, the local diffusion equation becomes $\partial_t f = D \partial_{JJ} f$. With these definitions, the particle loss rate at the collimator is equal to the flux at that location: $L = -D \cdot [\partial_J f]_{J=J_c}$. Particle showers caused by the loss of beam are measured with scintillator counters or ionization chambers placed close to the collimator jaw. The observed shower rate is parameterized as $S = kL + B$, where k is a calibration constant including detector acceptance and efficiency and B is a background term which includes, for instance, the effect of residual activation. Under the hypotheses described above, the diffusion equation can be solved analytically using the method of Green's functions, subject to the boundary condition of vanishing density at the collimator and beyond. Details are given in Ref. [27]. By using this diffusion model, the time evolution of losses can be related to the diffusion rate at the collimator position. With this technique, the diffusion rate can be measured over a wide range of amplitudes.

Some of the results of measurements in the Tevatron were presented in Refs. [17–19]. Experiments in the LHC were

reported in Ref. [2]. It was shown that the value of the diffusion coefficient near the core is compatible with measured emittance growth rates. The effect of collisions in both the Tevatron and in the LHC was clearly visible. In the Tevatron, diffusion enhancement in a specific amplitude region due to a hollow electron lens was observed. During the next run in 2015, we propose to measure halo diffusion in the LHC as a function of excitation strength in the transverse dampers, to provide a further test of the accuracy of the technique.

DISCUSSION AND CONCLUSIONS

Extracting beam distributions from collimator scrapings requires some care. The underlying assumption is that the beam distribution is static or that, if there is beam diffusion, it is independent of amplitude. In reality, the diffusion rate increases with betatron amplitude. Neglecting this fact results in overestimating the tails, and may explain in part the discrepancy between slow and fast scrapings in Ref. [1]. Another systematic effect is introduced by using a loss-monitor calibration that is independent of collimator position.

Van-der-Meer scans are used to measure the effective beam overlap and the absolute calibration of luminosity. Extracting from them a beam distribution and a halo population requires further hypotheses. The assumption that the two beams are identical introduces a systematic uncertainty.

It may be possible to get more accurate estimates of halo populations by taking into account the relationship between population density, diffusivity, and instantaneous loss rates from the diffusion model.

As an example, for simplicity, let us consider the Gaussian core of a beam with root-mean-square (rms), unnormalized emittance ε . In action coordinates, this translates into an exponential density $f_G(J, t) = (N/\varepsilon) \cdot \exp[-J/\varepsilon]$. Let's further assume a constant intensity decay, $N(t) = N_0 \exp(-\lambda t)$, and a constant emittance growth rate: $\varepsilon = \varepsilon_0 \exp(\gamma t)$. By multiplying the diffusion equation by J and integrating, one obtains a relationship between the emittance growth, the diffusion coefficient, and its gradient $D' \equiv \partial_J D$: $\gamma = 2 \langle (D/\varepsilon - D') \cdot J \rangle / \varepsilon^2$, where $\langle \rangle$ indicates an average over the distribution function. Moreover, by substituting the Gaussian form of the density f_G directly into the diffusion equation, one obtains a first-order differential equation for the diffusion coefficient:

$$D' - D/\varepsilon + \gamma \cdot J - (\lambda + \gamma)\varepsilon = 0 \quad (1)$$

It can be solved by imposing a null flux at the origin. This results in explicit forms for the diffusion coefficient as a function of action:

$$D(J) = \gamma \epsilon J + \lambda \epsilon^2 [\exp(J/\epsilon) - 1]. \quad (2)$$

In other words, an exponentially increasing diffusion coefficient is necessary to produce a Gaussian beam distribution. In more realistic cases (D increasing as a power of J), beam tails are inevitable.

These relationships can be used to test the stochastic model of halo dynamics and, if it is verified, to provide more accurate measurements of halo populations, which take diffusivity into account. One of the advantages of collimator scans is that they allow a simultaneous measurement of losses, drift velocities, and diffusivities as a function of betatron amplitude.

ACKNOWLEDGMENTS

This paper was based on the work of many people. In particular, the author would like to thank S. Redaelli, B. Salvachua, and G. Valentino of the LHC Collimation Working Group at CERN and G. Annala, T. R. Johnson, D. A. Still, and A. Valishev at Fermilab. W. Fischer, X. Gu (BNL), R. Bruce, H. Schmickler (CERN), N. Mokhov, T. Sen, V. Shiltsev (Fermilab), and M. Seidel (PSI) provided valuable insights.

REFERENCES

- [1] F. Burkart, Ph.D. Thesis, Goethe Universität, Frankfurt am Main, Germany, CERN-THESIS-2012-046 (2012).
- [2] G. Valentino et al., Phys. Rev. ST Accel. Beams **16**, 021003 (2013).
- [3] The CMS Collaboration, CMS-PAS-EWK-11-001 (2011).
- [4] S. Redaelli et al., in Proceedings of the 2013 International Particle Accelerator Conference (IPAC13), Shanghai, China, May 12–17, 2013, p. 978.
- [5] R. Schmidt et al., in Proceedings of the 2014 International Particle Accelerator Conference (IPAC14), Dresden, Germany, June 15–20, 2014, p. 1039.
- [6] B. Yee-Rendon et al., Phys. Rev. ST Accel. Beams **17**, 051001 (2014).
- [7] G. Stancari et al., FERMILAB-TM-2572-APC, arXiv:1405.2033 [physics.acc-ph], CERN-ACC-2014-0248 (2014).
- [8] A. J. Lichtenberg and M. A. Lieberman, *Regular and Chaotic Dynamics* (Springer-Verlag, New York, 1992), p. 320.
- [9] T. Chen et al., Phys. Rev. Lett. **68**, 33 (1992).
- [10] A. Gerasimov, FERMILAB-PUB-92-185 (1992).
- [11] F. Zimmermann, Part. Accel. **49**, 67 (1995); SLAC-PUB-6634 (1994).
- [12] T. Sen and J. A. Ellison, Phys. Rev. Lett. **77**, 1051 (1996).
- [13] K.-H. Mess and M. Seidel, Nucl. Instr. Meth. Phys. Res. A **351**, 279 (1994); M. Seidel, Ph.D. Thesis, Hamburg University, DESY 94-103 (1994).
- [14] L. Burnod, G. Ferioli, and J. B. Jeanneret, CERN-SL-90-01 (1990).
- [15] M. Meddahi, Ph.D. Thesis, Université de Paris VII, Paris, France, CERN-SL-91-30-BI (1991).
- [16] R. P. Filler III et al., in Proceedings of the 2003 Particle Accelerator Conference (PAC03), Portland, Oregon, USA, May 12–16, 2003, p. 2904.
- [17] G. Stancari et al., in Proceedings of the 2nd International Particle Accelerator Conference (IPAC11), San Sebastián, Spain, September 4–9, 2011, p. 1882, FERMILAB-CONF-11-411-AD-APC.
- [18] G. Stancari et al., in Proceedings of the 52nd ICFA Advanced Beam Dynamics Workshop on High-Intensity and High-Brightness Hadron Beams (HB2012), Beijing, China, September 17–21, 2012, p. 466, arXiv:1209.5380 [physics.acc-ph], FERMILAB-CONF-12-506-AD-APC.
- [19] G. Stancari et al., in Proceedings of the ICFA Mini-Workshop on Beam-Beam Effects in Hadron Colliders (BB2013), CERN, Geneva, Switzerland, March 18–22, 2013, CERN-2014-004, p. 83, arXiv:1312.5007 [physics.acc-ph], FERMILAB-CONF-13-054-APC.
- [20] G. Stancari et al., Phys. Rev. Lett. **107**, 084802 (2011).
- [21] G. Valentino et al., CERN-ATS-Note-2012-074-MD (2012).
- [22] N. Mokhov et al., J. Instrum. **6**, T08005 (2011).
- [23] D. Mirarchi et al., CERN-ACC-NOTE-2014-0061 (2014).
- [24] H. Schmickler, private communication (2014).
- [25] T. Mitsuhashi, in Proceedings of the 7th European Workshop on Beam Diagnostics and Instrumentation for Particle Accelerators (DIPAC05), CERN, Geneva, Switzerland, June 6–8, 2005, p. 7.
- [26] P. Thieberger et al., in Proceedings of the 2014 International Beam Instrumentation Conference (IBIC14), Monterey, California, USA, September 14–18, 2014, MOPD02.
- [27] G. Stancari, FERMILAB-FN-0926-APC, arXiv:1108.5010 [physics.acc-ph] (2011).